Investigating Completion Strategies—Cormorant Field, U.K. North Sea

Jess H. Stiles Jr., SPE, Esso E&P U.K. Ltd., and **Nicholas P. Valenti,** SPE, Exxon Production Research Co.

Summary. This paper describes studies by Esso E&P U.K. that evaluate various completion strategies for new subsea wells in the Cormorant field, U.K. North Sea. These studies, which complement work done by the field operator (Shell U.K. E&P), include detailed reservoir description work to define oil-in-place (OIP) and permeability distribution and a waterflood simulation for a representative reservoir cross section. Wellbore, flowline, and pipeline hydraulics for the complex production/injection system are included to model well rates more accurately. The results provide general insight into the nature of displacement during waterflooding of a stratified section with a limited number of wells. They also provide specific guidance on (1) dual vs. single completions; (2) perforating, testing, and stimulation sequence; and (3) the benefits of partially perforating high-permeability sands.

Introduction

The Cormorant field (Fig. 1) is 95 miles [150 km] northeast of the Shetland Islands at a depth of about 500 ft [152 m] in the U.K. North Sea. The field (Fig. 2), discovered in 1972, is composed of four major fault blocks that cover more than 10,000 acres [4×10^7 m^2] and contain more than 1.5 billion bbl [2.4×10^8 m^3] of oil. The field is a Shell/Esso joint venture and is operated by Shell U.K. E&P.

The southern portion of the field is developed from the South Cormorant platform and the northern area from the North Cormorant platform. Oil lying between the two platforms in Block I is being recovered with a sophisticated subsea-production system that consists of an Underwater Manifold Center (UMC)[1] and a single satellite well (Well P-1). Both the UMC and Well P-1 are connected to the South Cormorant platform by pipelines and control lines. All layers in the stratified reservoir section are being waterflooded concurrently by perforating all sands in both producer and injector wells. The permeability contrast among the sands is such that there is potential for severe imbalance in waterflood-front movement, resulting in large volumes of early water production from high-permeability layers and incomplete oil displacement from less permeable layers. With the high cost of expanding platform facilities or performing workovers on subsea wells to redistribute production and injection, there is considerable incentive to optimize completions in new wells. Completion of the UMC wells is the subject of this paper.

Block I

Block I (Fig. 3) is an elongated, westward-tilted fault block about 5,000 ft [1524 m] east/west and more than 45,000 ft [13 720 m] north/south that contains approximately 400 million bbl [64×10^6 m^3] of OIP. The structure, which dips at about 12 degrees, is truncated to the east and is bounded to the west by a limited aquifer. A major fault trending northeast/southwest divides the block roughly in half. The oil/water contact (OWC) is at −9,255 ft [−2821 m] to the north and at −9,180 ft [−2798 m] to the south. Although fluid contacts vary across the fault, the first wells drilled in the northern area showed pressure depletion, resulting from earlier production in southern wells. That indicated hydraulic communication across or around the fault. Many other faults have been identified from seismic and well data. Major reservoir characteristics are provided in Table 1.

Initial geologic and reservoir engineering studies indicated that good recovery could be achieved from Block I with a limited number of widely spaced producer and injector wells, with producers located west of the truncation surface and injectors just beyond the OWC. Development of the southern part of Block I began in 1980 with the drilling of wells from the South Cormorant platform. The major portion of the accumulation was not developed until 1983, however, when the UMC began production. Early UMC development was concentrated in the central portion of Block I with development in the north lagging because of the longer lead times needed for satellite-well (Wells P-5 and W-4) equipment to develop this area.

Producer Well P-5 and Injector Wells W-3 and W-4 were drilled during the winter of 1984–85 but were not scheduled for completion until the following summer because of weather considerations. Well P-5 had to be sidetracked twice before encountering the desired full section because the crestal area was more complex than originally mapped. A subsequent sidetrack may be required to deplete the complex crestal area fully once the downstructure area is depleted. Well W-3 was located just above the OWC to avoid faulting identified on seismic data.

The performance of early platform wells in Block I's southern portion indicated that the permeability contrast within the section was more severe than estimated from exploration-well log and core data and that high-permeability layers were being waterflooded very rapidly, resulting in large volumes of produced water. Production of excessive volumes of water is particularly undesirable for UMC wells because of the high cost associated with adding facility capacity to the South Cormorant platform and with performing workovers to alter the distribution of production and/or injection. (UMC workovers require a mobile rig, and the duration of workovers is extended by having to pull and then rerun the complex completion equipment.) It is also desirable to limit water production from UMC producers because of the adverse effects of water production on the hydraulics of the wells with long flowlines and pipelines. Scale formation also can occur once water production begins. As a result of these incentives to limit water production, we evaluated the potential for improving initial completions. Our objective was to find out how to reduce severe production and injection imbalances that might result in large volumes of early water production.

Fluid Properties. Block I is overpressured by more than 700 psi [4.8 MPa] and contains a 37°API [0.84-g/cm^3] -gravity oil. The 0.7-cp [0.7-mPa·s] oil results in a favorable mobility ratio. The oil is undersaturated by more than 2,700 psi [18.6 MPa], has a GOR of 480 scf/bbl [86.5 std m^3/m^3] and an initial oil FVF of 1.27 RB/STB [1.27 res m^3/stock-tank m^3]. Table 1 gives key reservoir fluid properties.

Geology. The oil at Cormorant field was accumulated in the deltaic sands of the Middle Jurassic Brent Group, located in the northern part of Block I. The Brent Group is divided into five productive formations, as shown in Fig. 4. These sands, from youngest to oldest, are the Upper Ness, Lower Ness, Etive, Rannoch, and Broom. The overall thickness of the section where the new wells are located is 200 to 250 ft [61 to 76 m] with a total net sand of 100 to 150 ft [30 to 46 m].

A detailed geologic study of the area formed the basis for reservoir engineering hand calculations and a simulation study that used a cross-sectional model. Several important conclusions resulted from the work. First, in addition to the Mid-Ness shale, there are laterally continuous shaly sections within and at the bases of the Lower Ness and the Rannoch that will prevent vertical fluid movement.

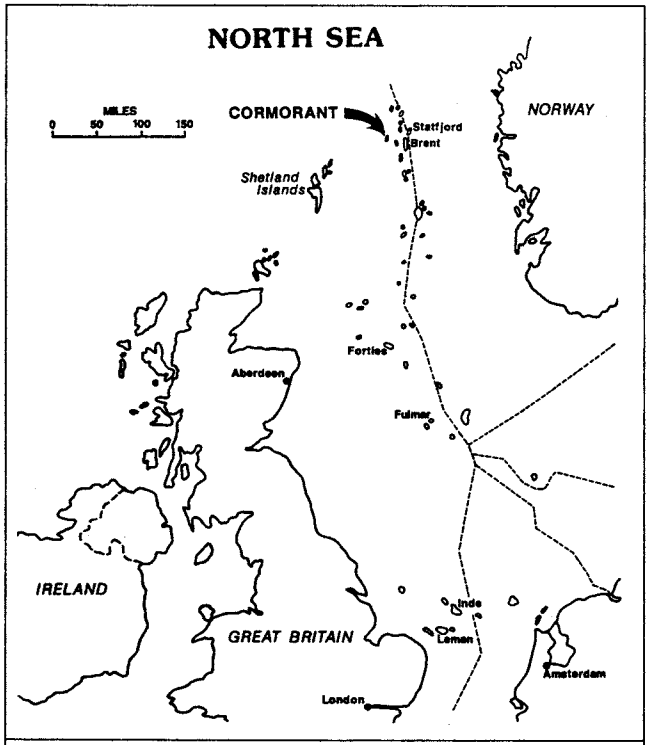

Fig. 1—Location of Cormorant field in the North Sea.

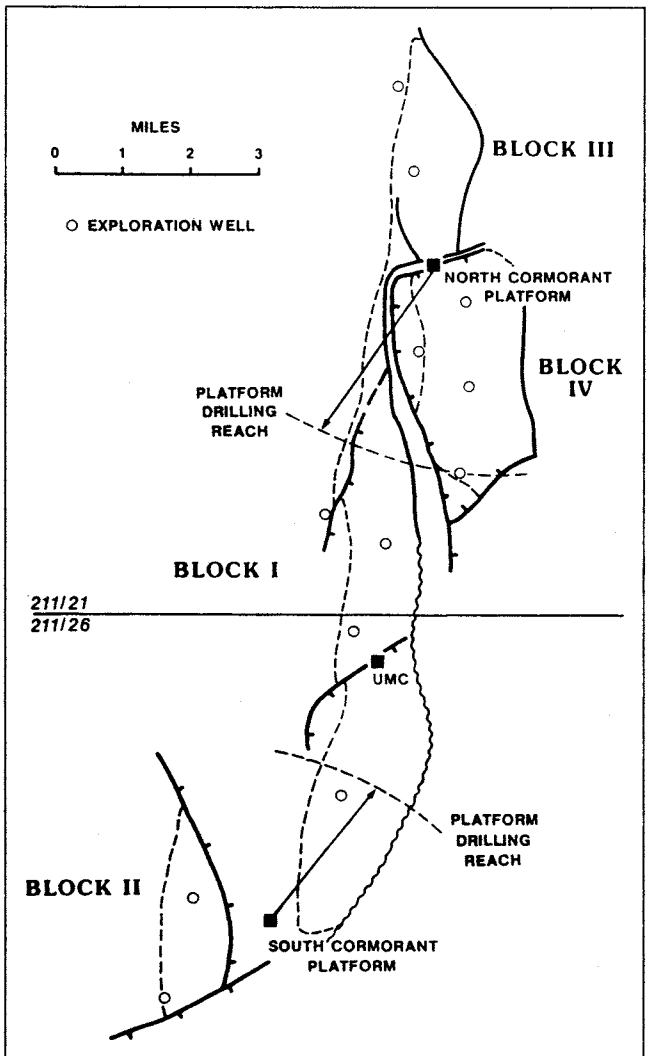

Fig. 2—Cormorant field map.

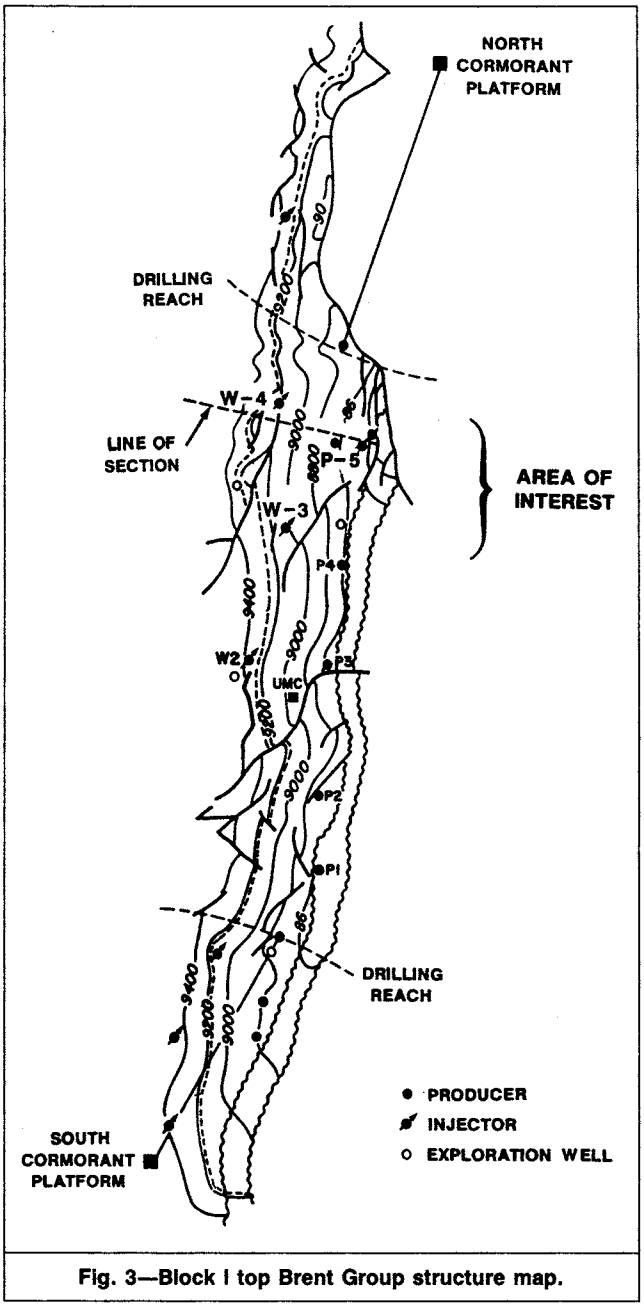

Fig. 3—Block I top Brent Group structure map.

TABLE 1—CHARACTERISTICS FOR BLOCK I RESERVOIR

Depth, ft subsea	8,750
p_i, psia	4,860
T_R, °F	215
Oil gravity, °API	37
GOR, scf/bbl	480
Bubblepoint, psia	2,100
B_{oi}, RB/STB	1.27
μ_{oi}, cp	0.72
OIP, million STB	400

There are also shaly intervals within the Upper Ness and Rannoch sands that, although creating localized flow restrictions, are judged unlikely to restrict vertical flow completely.

The geologic study confirmed the lateral and vertical continuity of the highly permeable Etive sands and concluded that the sands at the top of the Lower Ness (Lower Ness A) also have excellent lateral continuity and were potential paths for rapid water advance. The stratified nature of the section is supported by openhole-

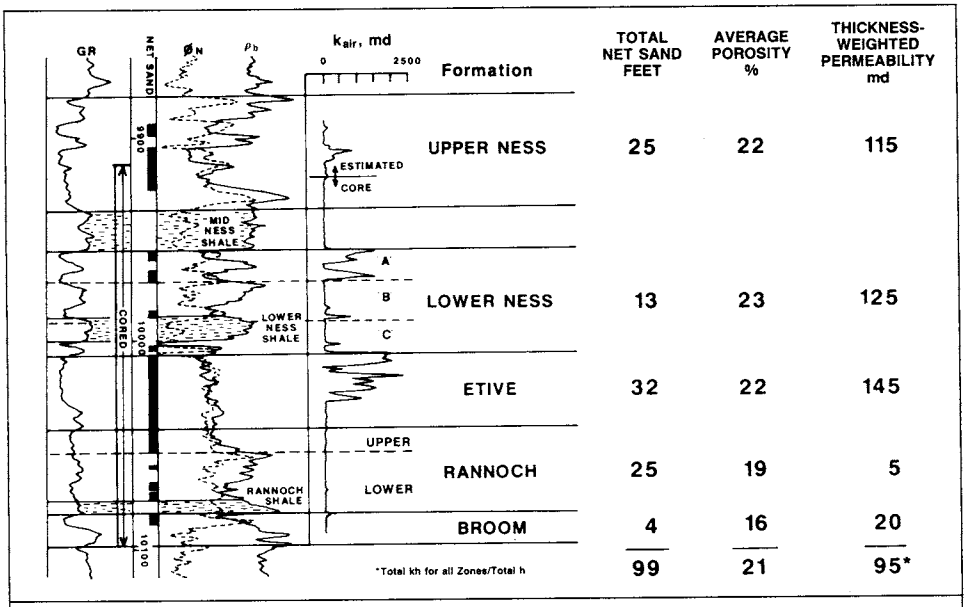

Fig. 4—UMC Well W-4 log.

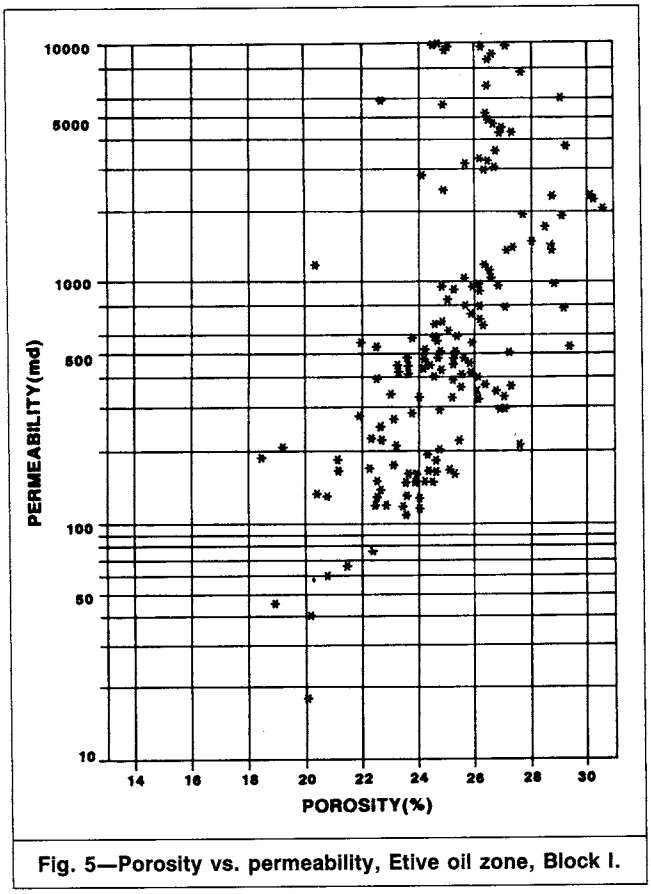

Fig. 5—Porosity vs. permeability, Etive oil zone, Block I.

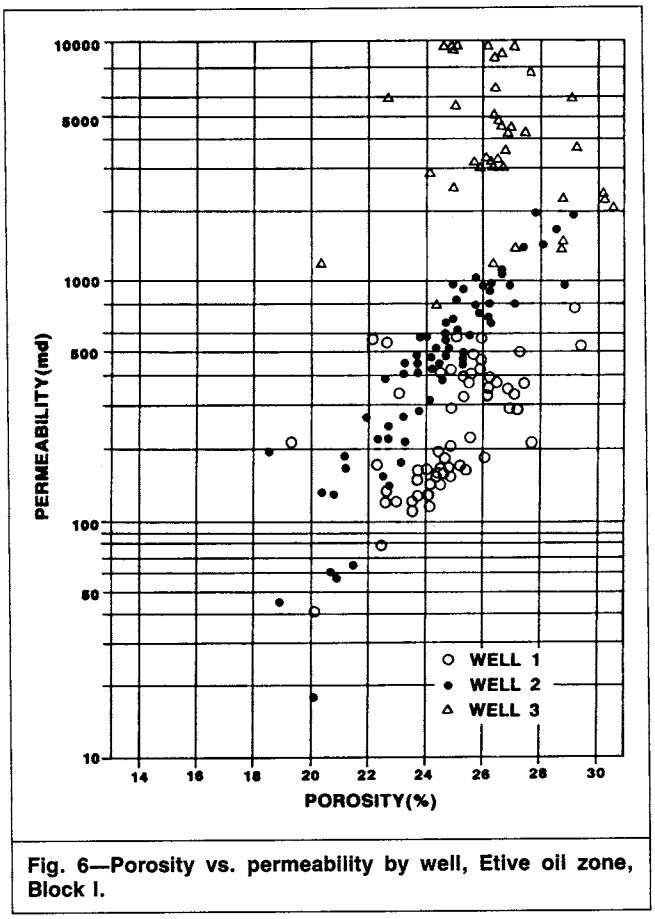

Fig. 6—Porosity vs. permeability by well, Etive oil zone, Block I.

formation-tester pressures, which showed significant variation throughout the section, resulting from earlier well production.

Refs. 2 through 4 discuss the geology of the Brent Group sands at Cormorant field in greater detail. Average rock properties are listed in Fig. 4. The permeability profile plotted in Fig. 4 shows the significant permeability contrast that exists within the section.

Permeability Distribution

A good understanding of permeability distribution is required to manage the reservoir correctly because, as previous studies of Cormorant field have shown, permeability distribution controls waterflood performance. Considerable effort was devoted to permeability distribution in this study with the use of extensive core data[4] from the central and northern areas of Block I. Core data were available for Wells W-3 and W-4, but it was necessary to predict permeabilities for Well P-5.

An often-used method is to define porosity-vs.-permeability relationships from core data for each major formation and then to use these relationships with log-calculated porosities to predict permeability. This method, however, was found to yield unacceptable results when tested in cored wells. Furthermore, efforts to correlate core permeability directly to a log response, or a group of log

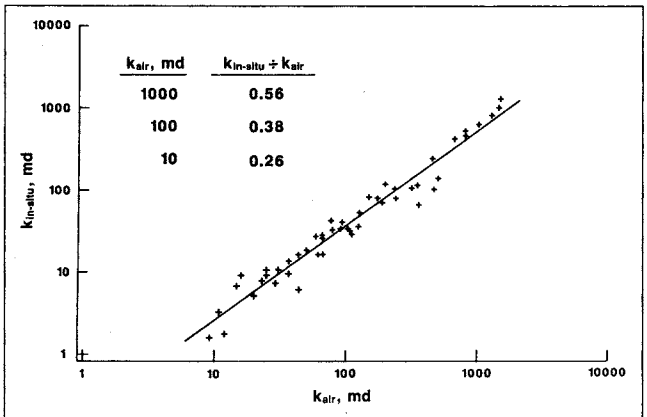

Fig. 7—Correction of routine core data for connate water and net overburden pressure.

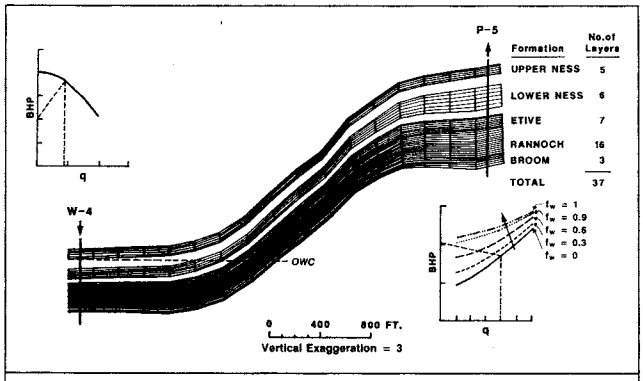

Fig. 9—Simulation cross section of Brent Group sands, northern UMC area. Large arrow denotes direction of increasing f_w.

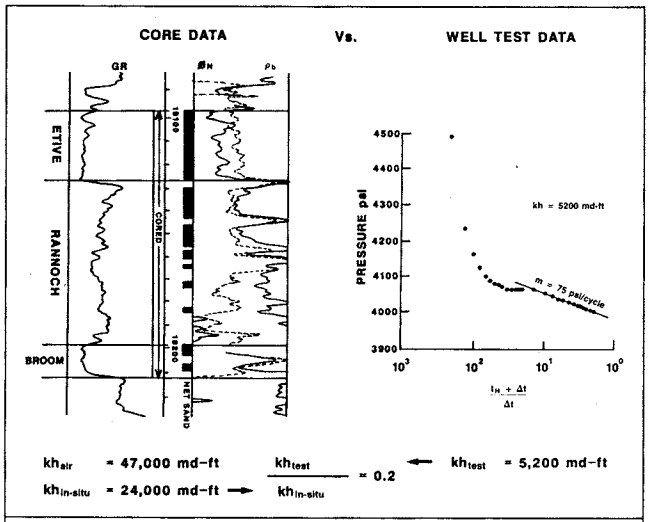

Fig. 8—Reconciliation of core data with test data, UMC injector Well W-2.

responses, also failed to yield acceptable results because of rock types with significantly different porosity/permeability relationships within the major formations. Fig. 5 shows an example porosity-vs.-permeability plot of Etive oil-zone core data from wells in the central and northern parts of Block I. If the significant scatter were randomly distributed, averaging might handle it acceptably. Closer examination of the data (Fig. 6), however, indicates that there are fairly well-defined trends for individual wells. Similar analyses in other parts of the Cormorant field show that similar differences exist within a single well.[4]

Although the potential to differentiate rock types from well log responses appears to exist, such an evaluation was beyond the scope of this study; therefore, an alternative approach was required. A nearby exploration well, Well 211/21-8, that correlates closely with Well P-5 had been fully cored. The Brent Group in Well 211/21-8 was divided into 28 layers to preserve the significant permeability contrast observed in the core data. With a detailed geologic correlation, we translated the permeabilities from Well 211/21-8 to Well P-5. However, permeabilities also had to be adjusted to account for the porosity differences in individual layers of the two wells.

It has been observed that permeabilities derived from routine core data are overstated at Cormorant field. As a result, the relationship shown in Fig. 7 was established from special core tests that corrected for the effects of connate water and overburden pressure. Significant corrections are defined for all permeability levels, but greater corrections were needed at lower permeabilities. The procedure's effect was to increase the permeability contrast within the section.

Once corrected for these effects, core data were reconciled with well-test results. Reconciliation is particularly important at Cormorant field, where there are instances of core permeability being enhanced as a result of the alteration of delicate clay structures during core preparation. The need for such further adjustment of core data was evaluated in the following way. A number of cored and tested Block I wells were selected for evaluation. These included wells from the oil and water zones. Core data over the tested interval were corrected for the effects of connate water saturation and net overburden pressure and then were summed to yield the total permeability-thickness product, *kh*. This value was compared to the *kh* value resulting from the analysis of pertinent well tests. The comparison indicated relatively good agreement for tested intervals in the oil column, with the corrected core data being only 16% higher, on average, than test data. There was poor agreement in the water zone, however. Results indicated that, on average, *kh* from corrected core data was three times the *kh* indicated from well tests. Fig. 8 is an example of the comparison made for a tested interval in Injector Well W-2.

This difference in *kh* values is consistent with the evidence that delicate clay structures exist in the rock within the water zone that are damaged during extraction and drying, thereby enhancing permeability above in-situ levels.[4-6]

Cross-Sectional Simulation Model

To evaluate various completion techniques, we constructed a 2D cross-sectional simulation model through the area to be waterflooded by Wells P-5 and W-4 (Fig. 9). The model section line is shown in Fig. 3. The model is composed of 37 layers with 22 blocks in the dip direction for a total of 814 gridblocks. The width of the model was selected to approximate the average producer and injector spacing (about 4,000 ft [1219 m]) in the northern portion of Block I. The model includes a producer and an injector at the locations of Wells P-5 and W-4.

Wellbore and flowline hydraulics provided by Shell, shown as inserts in Fig. 9, were used to define well rates. These curves, which are based on assumptions of average flow rates from all UMC wells, include the hydraulics effects of the common pipelines from the South Cormorant platform to the UMC, the satellite flowlines from the UMC to Wells P-5 and W-4, and the two 3½-in. [9-cm] tubing strings that are installed in UMC wells to allow through-flowline (TFL) techniques to be used for well monitoring and maintenance.

Porosities were assigned on the basis of core data corrected for net overburden pressure. Where core data were not available, log-calculated porosities were used. Irreducible water saturations were defined for the various rock types with Shell's log calculations.

Relative permeabilities were based on waterflood tests conducted at reservoir conditions on core material with natural wettability preserved. Because this information was not yet available for Cormorant field, relative permeability data for a nearby field that produces similar oil from the Brent Group sands were used. Com-

TABLE 2—EFFECTS OF CORE ANALYSIS AND VISCOSITY ADJUSTMENTS

Basis	Injectivity Index (B/D-psi)	Injection Rate (B/D)
Routine core analysis	146	20,000
Special core analysis correction	89	19,000
Effect of cold-water injection	19	15,000
Well-test reconciliation	6	9,000

parative tests in other Brent Group reservoirs indicated that coring fluid, preservation, and test procedures can have a very significant effect on relative permeabilities.[7]

Although the water viscosity initially assigned to the model corresponded to initial reservoir conditions, it was necessary to adjust it with time to approximate reservoir cooling around the injector. The timing and areal extent of water viscosity adjustments were based on previous thermal simulation work. Results of this work indicated that the long-term injectivity effect is roughly equivalent to using the cold seawater viscosity within the radius of investigation of the well. (The thermal front was calculated to extend up to 1,500 feet [457 m] from the injector; the distance varied depending on the permeability of each zone and adjacent beds.)

Table 2 shows the effects of the various core data corrections and adjustments and of the cold seawater injection. Overall, the injectivity index is reduced by a factor >20 and the injection rate by a factor >2. The impact is smaller on the injection rate because it is controlled largely by wellbore and flowline hydraulics and not by the injectivity index.

Nonselective Production and Injection

Maximum production and injection can be achieved by fully perforating all sands and by using both tubing strings to inject into the entire reservoir section. This was the initial case evaluated. In such a case, production and injection are distributed among layers primarily on the basis of *kh*. The results showed that the high-permeability Lower Ness A and Etive sands are waterflooded at a very rapid rate. Water breakthrough occurs within about 2 years, with the subsequent production of large volumes of water. Fig. 10 shows the waterflood-front locations in the various layers at breakthrough.

Fig. 11 shows the water-breakthrough timing and the subsequent increase in water cut for individual layers of the base case. The Lower Ness A and Etive sands are flooded very rapidly, with the remaining layers lagging substantially.

To help explain these results, Table 3 compares the *kh* distribution in Well P-5 with the OIP in the entire model. The ratio of the *kh* fraction to the corresponding OIP fraction within each waterflood interval is also included in Table 3. For a well-balanced waterflood, the values would be near 1.0; i.e., the *kh* distribution, which controls production and injection distribution, would match the OIP distribution. Table 3 shows severe imbalances, however, because the Lower Ness A and Etive sands have excessive *kh* relative to their OIP and all remaining layers have inadequate *kh*. Other Lower Ness sands also show *kh* imbalance in Well P-5 resulting from the localized thickening of a highly permeable sand at the formation

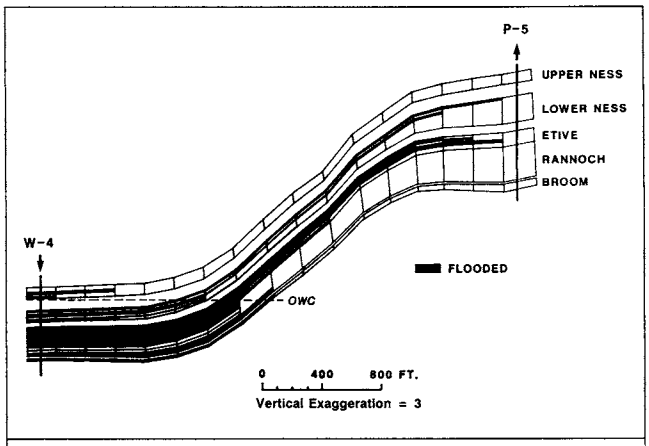

Fig. 10—Location of waterflood front at breakthrough, fully perforated case.

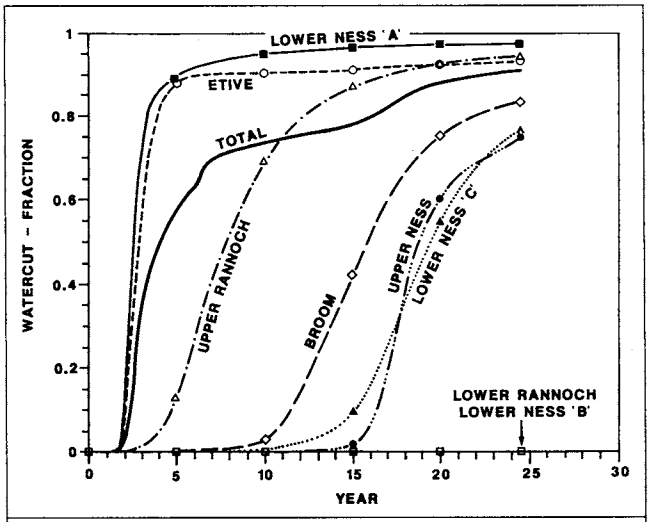

Fig. 11—Individual sand water cut vs. time, fully perforated case.

base. This does not occur in Well W-4 or elsewhere in the northern portion of Block I, however, and when the entire area is considered, these sands have a *kh* deficiency relative to their OIP.

Table 3 also indicates that the high-permeability Etive and Lower Ness A sands contain <30% of the model OIP. Consequently, unrestricted waterflooding of these sands will result in a large part of the total recovery from this area of the field being produced at high water cut. Thus, there is an incentive to seek improved reservoir performance.

The importance of the less-permeable Upper Ness sand is demonstrated in Fig. 12, which shows the oil recovery from individual sands vs. time. About 4 million bbl [6×10^5 m^3] of oil is recovered from the Upper Ness formation, a volume that exceeds that recovered from the high-quality Etive sands. Water breakthrough

TABLE 3—OIP AND *kh* DISTRIBUTION IN WELL P-5

Interval	*kh* in Well P-5 md-ft	*kh* in Well P-5 % of Total	OIP (% of Total)	*kh*/OIP (fraction)
Upper Ness	2,000	9	26	0.3
Lower Ness A	3,100	14	8	1.8
Other Lower Ness	4,700	20	12	1.7
Etive	9,500	41	20	2.0
Rannoch	3,500	15	31	0.5
Broom	300	1	3	0.3
Total	23,100	100	100	1.0

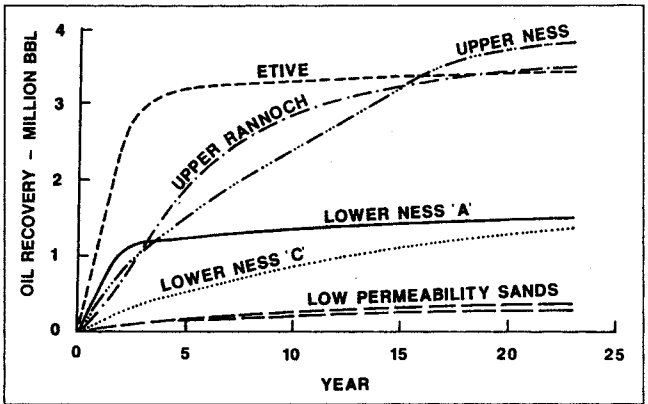

Fig. 12—Individual sand oil recovery vs. time, fully perforated case.

occurs late in the Upper Ness field life, even assuming an undamaged wellbore. In a number of instances in Cormorant, drilling injectors with oil-based mud has resulted in wellbore damage, and stimulation diversion has not always been successful in removing such damage. The above simulation results indicate a need to ensure that less-permeable intervals, such as the Upper Ness, are tested and, if necessary, stimulated before the high-permeability sands are perforated.

Dual Completions

One alternative technique to improve relative flood-front velocities in individual layers is to control fluid distribution by use of dual completions. This allows injection into part of the restricted section. Effective flow segregation requires that a packer be set in the wellbore opposite a reasonably thick, laterally extensive shale. (Although UMC wells are equipped with two 3½-in. [9-cm] tubing strings for TFL application, they are not routinely equipped with a second packer to segregate flow between the strings.) Shales with continuity over the northern part of Block I were identified in the geologic study and are shown in Fig. 4.

We considered two aspects in evaluating the benefits of selective completions. The first concerns the balance between OIP and *kh*. OIP and *kh* distributions, shown in Table 3, indicate that dually completing Well P-5 across a shale within or at the base of the Lower Ness would do little to improve this imbalance. The Lower Ness A would still be flooded preferentially in the upper tubing string, whereas the Etive would be flooded preferentially in the lower tubing string. Indeed, simulation results showed little improvement in waterflood performance with segregated tubing strings.

Greater improvement could be achieved by placing the packer at the Mid-Ness shale, but our second consideration—the effect on production and injection rate—had to be addressed. Maximum rate is achieved with nonselective production or injection through both tubing strings. Dedicating each string to a part of the reservoir interval can result in a significant rate reduction. The combined injection rate for selective completions above and below the Mid-Ness shale in Well W-4 was calculated from hydraulics curves and found to be just over 7,000 BWPD [1113 m^3/d water] vs. almost 9,000 BWPD [1431 m^3/d water] for a nonselective completion. Thus, selective completions reduced rates by about 17%. Such an injection-rate reduction results, in turn, in a reduced oil rate from Well P-5 caused by lack of pressure support. Selective injection has the added risk of the injection rate being much lower than expected because of inaccuracies in estimating permeabilities for the various layers, with a very expensive workover being required to alter the completion configuration should the actual injection rate be unacceptable.

We concluded that there was little incentive for selective production and/or injection in Wells P-5 and W-4 because the high-permeability layers are not grouped appropriately. Having the high-permeability sands grouped either at the top or the bottom of the reservoir section would offer the best opportunity for improving overall waterflood performance with selective completions. Such a situation is not normally encountered at Cormorant field because of the depositional sequence.

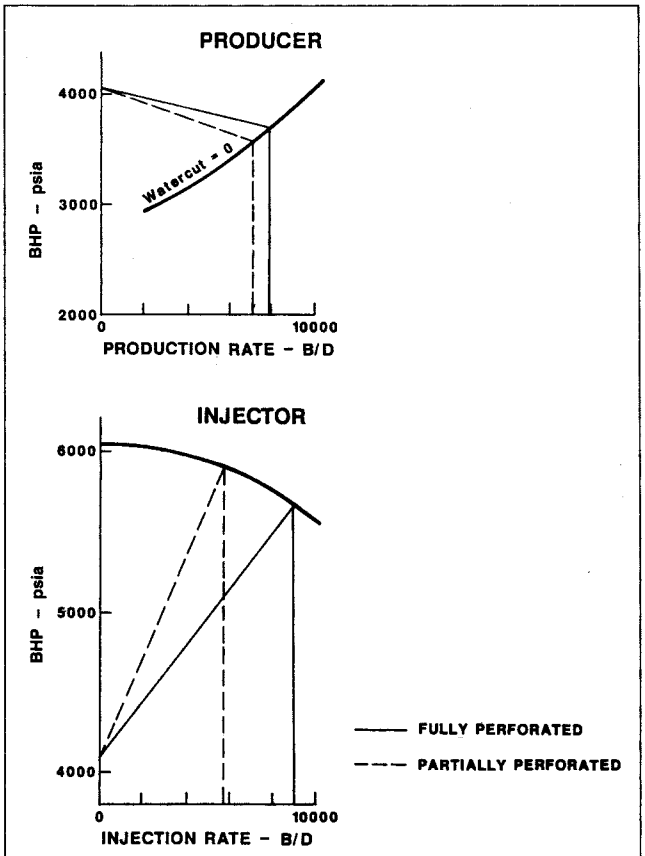

Fig. 13—Comparison of initial well rates, fully vs. partially perforated producer and injector.

Partial Perforation

Another alternative we considered was to alter the production or injection distribution by only partially perforating the wells—i.e., by effectively reducing the *kh* of the high-permeability sands at the wellbore. This technique, which has been used successfully in North Cormorant platform wells, avoids the problems of selective injection as discussed earlier.

The cross-sectional model was rerun with the wellbore *kh* of the Lower Ness A and the Etive sands reduced to improve production balance. This was modeled by perforating only 2 ft [0.6 m] in each of the thin Lower Ness A sands and by perforating only the uppermost Etive layer in Well P-5. We would have preferred to reduce the *kh* of the Lower Ness A further on the basis of the imbalance shown in Table 3. A 2-ft [0.6-m] perforation was considered the minimum acceptable, however, because we were concerned that perforating only 1 ft [0.3 m] of a thin interval might result in an overly reduced rate. Moreover, adding perforations later would necessitate an extension to the already long completion time or a short, but nonetheless expensive, re-entry at a later date.

Preliminary simulation runs and wellbore-hydraulics calculations indicated an advantage in partially perforating the upstructure producer, which was expected to have excellent productivity because of higher permeability and low oil viscosity. This is not true for the downstructure injector, where injectivity would be severely limited because of clay mineralogy and the increased viscosity of cold injection water.

Limiting perforations in the injector resulted in lower overall production rates from the model because of the lack of pressure support. Fig. 13 shows the procedure for the hydraulic rate calculations, and Table 4 summarizes the results.

Fig. 14 compares water-cut profiles from the simulation cases with fully and partially perforated producers. Although the water-

TABLE 4—PARTIAL PERFORATION STRATEGY

Well	Initial Rate (1,000 B/D) Fully Perforated	Partially Perforated	Reduction (%)
Producer P-5	7.9	[7.1*]	10
Injector W-4	[8.9*]	5.7	36

*Strategy for balanced waterflood.

breakthrough time is about the same in the two cases, the partially perforated case resulted in an improvement in overall water-cut performance. The water cut is lower until late in the field life. Water breakthrough occurs at about the same time because production from the thin Lower Ness A cannot be restricted to the same extent as from the thicker Etive because of the practical limitation described earlier.

The improved waterflood efficiency is confirmed in Fig. 15, which compares water cut vs. recovery for the two cases. Examination of the full results showed the following overall improvements in waterflood efficiency: (1) oil recovery at a 90% terminal water cut increased by 300,000 bbl [47 696 m^3]; (2) the total volume of produced water was reduced from 23 to 20 million bbl [3.7×10^6 to 3.2×10^6 m^3]; and (3) the total amount of water injected was reduced from 42 to 39.5 million bbl [6.7×10^6 to 6.3×10^6 m^3]. The higher oil recovery results from increased waterflood throughput in the poorer-quality rock with little offsetting effect in the high-permeability sands, which are subjected to large throughputs in either case.

Although partial perforating results in initial rates that are about 6% lower, this is compensated for by higher oil rates after water breakthrough and lower water cut during much of the field life.

Application to Well W-3

Although Well W-3 was not included in the cross-sectional model, results of the model studies were valuable to formulate its completion policy. Core-data analysis was used to calculate an expected injection distribution if the entire section were perforated, and this distribution was compared with the OIP distribution in this area of the field (Table 5). We grouped a portion of the Upper Rannoch with the Etive in this analysis because the Upper Rannoch is being well developed and is judged to be in good vertical communication with the Etive. The fourth column in Table 5 shows that 44% of the injection would go into the Lower Ness A if all intervals were perforated fully. The second column indicates that this sand contains only about 8% of the OIP. The *kh* product and a fraction of total well *kh* are higher in Well W-3 than in Well W-4, located to the north, because of a combination of higher permeability and increased sand thickness. As a result, only 3 ft [1 m] of the 20-ft [6-m] -thick interval in the Lower Ness A was perforated. This was calculated to reduce the injection rate into that interval by about 45% and to reduce the initial injection rate for the total well by $<10\%$.

Additionally, the high-permeability Lower Ness A and Etive sands were perforated only after the intervals with poorer permeabilities were perforated, tested, and stimulated. The distribution actually achieved was measured by a flowmeter, and results are shown in the last column in Table 5. Although the actual distribution does not mirror the OIP exactly, it represents an improvement over the distribution that would have resulted had all layers been perforated fully.

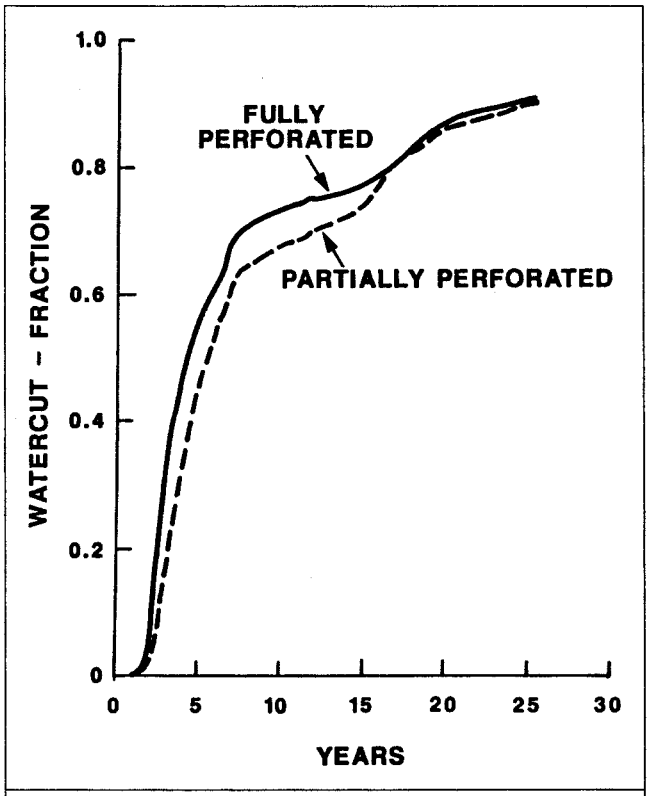

Fig. 14—Water cut vs. time, fully and partially perforated producer.

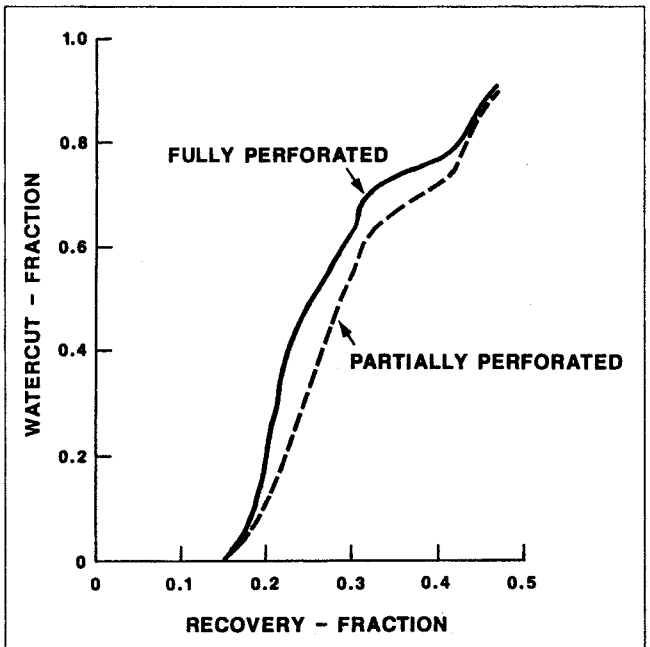

Fig. 15—Water cut vs. recovery, fully and partially perforated producer.

Conclusions

There is potential to improve waterflood efficiency in the UMC area of Cormorant's Block I through detailed reservoir description and simulation studies. Integration and reconciliation of data from numerous sources are required to do this. Specific conclusions of our work follow.

1. A good understanding of the permeability distribution is critical. Full use should be made of core analysis results, and techniques should be developed to predict permeabilities in uncored wells more accurately. Routine core data have to be corrected to in-situ conditions and reconciled with well-test results. We had good agreement between corrected core data and well tests in the oil zone, but a large adjustment was needed for core data from the water zone.

2. Wellbore, flowline, and pipeline hydraulics and the effects of injecting cold seawater need to be included in the waterflood simulation to determine the effects of various completion alternatives on field performance correctly.

TABLE 5—IMPROVED INJECTION DISTRIBUTION OF WELL W-3

Interval	OIP (%)	Perforation Sequence	Injection Distribution (% of Total) Fully Perforated, Estimated	Partially Perforated, Actual
Upper Ness	15	1	5	15
Lower Ness A	10	2	44	6
Other Lower Ness	10	1	4	15
Etive/Upper Rannoch	53	2	47	62
Lower Rannoch	8	1	0	0
Broom	4	1	0	2
Total	100	—	100	100

3. When high-permeability sands are distributed throughout the reservoir section rather than grouped together, there is little justification for dual completion of the wells by use of an additional packer to improve the production and/or injection distribution.

4. We identified potential waterflood-performance improvements by partially perforating high-permeability sands. Improvements were increased oil recovery at the terminal water cut, reduced water production, and reduced water injection. These were accomplished with only a slight reduction in initial production and/or injection rates.

5. A large proportion of the final oil recovery is from intervals with lower permeabilities, and recoveries from such sands could be jeopardized if they are damaged at the wellbore. Therefore, these sands should be perforated, tested, and stimulated, if necessary, before high-permeability intervals are perforated.

6. Actual flow distributions measured with flowmeters following well completion indicate that the above techniques can be effective in improving flow distributions. The simulation results indicate that this can lead, in turn, to improvements in waterflood efficiency.

Nomenclature

B_{oi} = initial oil FVF
f_w = water fractional flow
h = thickness, ft [m]
k = permeability, md
k_{air} = routine air permeability, md
$k_{in\text{-}situ}$ = in-situ permeability, md
m = slope, psi/cycle [kPa/cycle]
p_i = initial pressure, psi [kPa]
q = flow rate
Δt = shut-in time, hours
t_H = Horner time, hours
T_R = reservoir temperature, °F [°C]
μ_{oi} = initial oil viscosity, cp [Pa·s]
ρ_b = bulk density, g/cm^3
ϕ_N = neutron porosity

Acknowledgments

We thank Shell U.K. E&P for permitting us to publish this paper. We also thank the managements of Esso E&P U.K. and Exxon Production Research Co. for the opportunity to prepare it. We also acknowledge T.C. Boberg, who supervised the reservoir description and simulation work.

References

1. Childers, T.W., Verhaak, T.A., and Loth, W.D.: "UMC Design Review," *Proc.*, 15th Offshore Technology Conference, Dallas (1983) **3**, 245–56.
2. Watters, D.G., Pagan, M.C.T., and Provan, D.M.J.: "Cormorant Field, UK North Sea: Synergistic Approach to the Optimum Development of a Complex Reservoir," *Proc.*, AAPG Annual Meeting, New Orleans (March 24–27, 1985).
3. Budding, M.C. and Inglin, H.F.: "A Reservoir Geological Model of the Brent Sands in Southern Cormorant," *Petroleum Geology of the Continental Shelf of Northwest Europe*, Heyden & Son Ltd., London (1981) 326.
4. Stiles, J.H. and McKee, J.W.: "Cormorant: Development of a Complex Field," paper SPE 15504 presented at the 1986 SPE Annual Technical Conference and Exhibition, New Orleans, Oct. 5–8.
5. de Waal, J.A. *et al.*: "Petrophysical Core Analysis of Sandstones Containing Delicate Illite," paper Z presented at the 1986 SPWLA European Formation Evaluation Symposium, Aberdeen, April 23–25.
6. Heaviside, J., Langley, G.O., and Pallatt, N.: "Permeability Characteristics of Magnus Reservoir Rock," paper A presented at the 1983 SPWLA European Formation Evaluation Symposium, London, March 14–15.
7. Stiles, J.H. Jr. and Hutfilz, J.M.: "The Use of Routine and Special Core Analysis in Characterizing Brent Group Reservoirs, U.K. North Sea," paper SPE 18386 presented at the 1988 SPE European Petroleum Conference, London, Oct. 16–19.

SI Metric Conversion Factors

°API	141.5/(131.5+°API)		=	g/cm^3
bbl	× 1.589 873	E−01	=	m^3
cp	× 1.0*	E−03	=	Pa·s
ft	× 3.048*	E−01	=	m
°F	(°F−32)/1.8		=	°C
md	× 9.869 233	E−04	=	μm^2
miles	× 1.609 344*	E+00	=	km
psi	× 6.894 757	E+00	=	kPa
scf	× 2.863 640	E−02	=	std m^3

*Conversion factor is exact.

SPEFE

Original SPE manuscript received for review Sept. 8, 1987. Paper accepted for publication Sept. 26, 1989. Revised manuscript received Jan. 6, 1989. Paper (SPE 16553) first presented at the 1987 SPE Offshore Europe Conference held in Aberdeen, Sept. 8–11.